Generation of Fluorescence Quenchers from the Triplet States of Chlorophylls in the Major Light-Harvesting Complex II from Green Plants†

Virginijus Barzda,*,‡ Mikas Vengris,‡,§ Leonas Valkunas,§ Rienk van Grondelle,‡ and Herbert van Amerongen‡

Faculty of Sciences, Division of Physics and Astronomy, Vrije Universiteit, De Boelelaan 1081, 1081 HV Amsterdam, The Netherlands, and Institute of Physics, A. Gostauto 12, LV2600 Vilnius, Lithuania

Received December 9, 1999; Revised Manuscript Received June 26, 2000

ABSTRACT: Laser flash-induced changes of the fluorescence yield were studied in aggregates of light-harvesting complex II (LHCII) on a time scale ranging from microseconds to seconds. Carotenoid (Car) and chlorophyll (Chl) triplet states, decaying with lifetimes of several microseconds and hundreds of microseconds, respectively, are responsible for initial light-induced fluorescence quenching via singlet−triplet annihilation. In addition, at times ranging from milliseconds to seconds, a slow decay of the light-induced fluorescence quenching can be observed, indicating the presence of additional quenchers generated by the laser. The generation of the quenchers is found to be sensitive to the presence of oxygen. It is proposed that long-lived fluorescence quenchers can be generated from Chl triplets that are not transferred to Car molecules. The quenchers could be Chl cations or other radicals that are produced directly from Chl triplets or via Chl triplet-sensitized singlet oxygen. Decay of the quenchers takes place on a millisecond to second time scale. The decay is slowed by a few orders of magnitude at 77 K indicating that structural changes or migration-limited processes are involved in the recovery. Fluorescence quenching is not observed for trimers, which is explained by a reduction of the quenching domain size compared to that of aggregates. This type of fluorescence quenching can operate under very high light intensities when Chl triplets start to accumulate in the light-harvesting antenna.

Under high light conditions, the photosynthetic apparatus becomes oversaturated, leading to an enhancement of photoinhibition and increase of triplet production (*1*). The triplet excited state of chlorophyll (Chl)[1] can be very effective in generating singlet oxygen, which is a lethal damaging agent for living organisms (*2*). Plants have developed several protective mechanisms to lower the concentration of Chl triplets. Carotenoids (Cars), which are in close contact with Chl in the light-harvesting antennae, very efficiently accept the Chl triplets (*3*). Car triplets do not generate singlet oxygen and can even quench it, thus serving as a double protector for Chl and other molecules against oxidation (*4*). In light-harvesting antennae of most photosynthetic organisms, close to 100% of the Chl triplets is transferred to Car. Recently it was found (*5*) that in aggregated as well as in trimeric light-harvesting chlorophyll *a*/*b* pigment−protein complex of photosystem II (LHCII) isolated according to the method described in (*6*) 92 ± 7% of the Chl triplets are transferred to Car at room temperature. This showed that in LHCII not all Chls have neighboring Cars.

In addition to fast Chl triplet transfer to Car, plants have developed another strategy to reduce the concentration of Chl triplets. Under high light intensities, quenchers of singlet excitations are generated in photosystem II (*7*). At least part of these quenchers appears in the light-harvesting antennae and are responsible for a protective mechanism known as nonphotochemical quenching (*7*). Despite the fact that the origin of this mechanism remains unclear, there is common agreement about the correlation of the quenching with a pH gradient across the membrane. Correlation between nonphotochemical quenching and the xanthophyll cycle has also been established (for reviews, see refs *1* and *8*).

To understand the mechanism of nonphotochemical quenching, one must understand fluorescence quenching in general and light-induced quenching specifically. The study of the mechanism and time scale of light-induced generation of the fluorescence quenchers in isolated LHCII will be presented in this work. The light-induced fluorescence quenching (ΔF) in isolated LHCII was first observed by Jennings et al. (*9*). It was shown that the fluorescence yield of LHCII macroaggregates drops by 10−25% under strong illumination and then recovers on a ∼50 s time scale. Kinetics of ΔF were sensitive to the xanthophyll and lipid content in LHCII (*10*, *11*). It was shown (*12*) that LHCII preparations containing only major LHCII exhibited a larger ΔF than preparations contaminated by minor antenna complexes. Detailed investigations of the kinetics (on a time scale of seconds) of ΔF have been performed (*13*), demonstrating the dependence

† V.B. was supported by an EMBO fellowship ALTF 131-1996 and by a visitors grant from the Dutch Foundation for Scientific Research (NWO); M.V. was financed by the EU TEMPUS program (TEMPUS MJEP-09700-95).

* To whom correspondence should be addressed. New address: Department of Chemistry and Biochemistry, University of California, San Diego, 9500 Gilman Drive, Department 0339 La Jolla, CA 92093-0339. Phone: (858) 534-0290. Fax: (858) 534-7654. E-mail: vxb@chem.ucsd.edu.

‡ Vrije Universiteit.

§ Institute of Physics.

[1] Abbreviations: Car, Carotenoid; Chl, chlorophyll; CMC, critical micelle concentration of the detergent; DM, *n*-dodecyl β-D-maltoside; FWHM, full width at half-maximum; LHCII, light-harvesting chlorophyll a/b pigment−protein complex of photosystem II; ΔF, light-induced reversible fluorescence quenching; MCP, microchannel plate photomultiplier; T−S, triplet minus singlet.

10.1021/bi992826n CCC: $19.00
Published on Web 08/04/2000

of this phenomenon on the state of aggregation, temperature, and light intensity. It was revealed that the rate of quencher formation linearly depends on the light intensity (*9*, *13*). The slow decline in fluorescence was determined by the low concentration of excited states, however, the process of quencher generation appeared to be fast, in the order of the lifetime of the excited states. Meanwhile, the disappearance of light-induced quenchers turned out to be a thermally activated reaction, involving large entropy changes. The amount of fluorescence quenching decreases upon desaggregation with a characteristic larger decrease around the critical micelle concentration (CMC) of the detergent.

In this study, we investigate the generation of the light-induced fluorescence quenchers by time-resolved fluorescence after excitation of Chls in LHCII with powerful nanosecond laser pulses. The kinetics of ΔF are shown to be sensitive to the presence of oxygen. Modeling of the ΔF kinetics under aerobic and anaerobic conditions reveal that fluorescence quenchers can be generated from Chl triplet states. This indicates the presence of a protective mechanism with a negative feedback which lowers the generation of Chl triplets once a Chl triplet mediated fluorescence quencher has been generated in the domain. This mechanism becomes significant at high light intensities when Chl triplets start to accumulate in the light-harvesting antennae.

EXPERIMENTAL PROCEDURES

Sample Preparation. LHCII aggregates were isolated from leaves of 2 week-old pea (*Pisum sativum*) plants as described in ref *6*. A lamellar type of LHCII macroaggregates was used in this study. The LHCII was stored in a 15 mM Tricine/NaOH, pH 7.8, buffer at 4 °C and used within 2 weeks after isolation. Anaerobic conditions were obtained by degassing the sample under reduced pressure and flushing it subsequently with nitrogen (*14*, *5*). The amount of oxygen present in the sample was estimated from the lifetime of Car triplets ranging from 9 to 3 μs under anaerobic or oxygen saturated conditions, respectively (*15*). For desaggregation of LHCII aggregates *n*-dodecyl β-D-maltoside (DM) was used. The critical micelle concentration (CMC, the concentration at which LHCII aggregates are disassembled into trimers) of DM for this type of LHCII preparation was about 0.009% (w/v). A concentration of 10 μg/mL chlorophyll was used and all the measurements were performed in acrylic cuvettes with an optical path length of 1 cm. An Oxford Instruments DN1704 liquid nitrogen bath cryostat was used for experiments at 77 K. For the low-temperature studies, the sample was suspended in a mixture of $^1/_3$ buffer + $^2/_3$ glycerol (volume).

Laser-Flash Induced Fluorescence Transients. The measurements of laser flash-induced fluorescence transients were performed under aerobic and anaerobic conditions with a home-built setup. The light-induced quenchers were generated by 8 ns (full width at half-maximum, FWHM), 590 nm, and 10 mJ laser pulses from a dye laser (Quanta Ray PDL2, dye: Rhodamine 6G), which was pumped by a frequency-doubled Q-switched Nd:YAG laser (Quanta Ray DCR2). The fluorescence was collected at 90° with respect to the excitation and probing beam. The probing light and detection system was organized in two ways, depending on the time scale. On a time scale from 5 μs to 2.2 ms the experiments were performed with a fast side-window photomultiplier (Hamamatsu R928), by probing with the xenon lamp in a flash mode (flash duration of about 5 ms). On longer time scales, from 5 ms to 18 s, the fluorescence was measured with a more sensitive front window photomultiplier (Thorn-EMI 9658) while the sample was continuously illuminated by the probing light. In both cases, the probing light intensity was kept as low as possible, to prevent quencher generation. The scattered light was eliminated using a band-pass filter (type C3C-22, transmission maximum at ~450 nm, ~100 nm band width) for the probing beam and a cutoff filter (KC-19, cutting at 700 nm) for the detection. In both cases, the time resolution of the experiment was limited by the photomultiplier recovery time after the strong spike of the prompt fluorescence induced by the laser pulse. The recovery times of the photomultipliers were investigated using a scattering sample and the red filter removed or Rhodamin 6G in methanol as a sample. The instrument response time was 4.3 μs for the fast time scale arrangement and 4 ms for the slow time scale. The signals were recorded and averaged with a 300 MHz band width digital oscilloscope (LeCroy 9310) and transferred to the computer for processing afterward. To avoid the accumulation of long-lived quenchers [which disappear in about 20 s (*13*)] and irreversible light-induced changes, the sample was changed every 32 laser shots, keeping accumulated fluorescence changes below the noise level. For the same reason, the repetition rate of the laser pulses was lower than one pulse per 30 s. The sequence of the measurements was as follows: first the sample fluorescence was recorded before each laser pulse, using probe light. Then the laser pulse was applied to the sample and the fluorescence changes were recorded for a certain period. The signal was then normalized to the "dark" fluorescence.

Time-Correlated Single Photon Counting. Fluorescence lifetime measurements were performed using the time-correlated single photon counting technique (see ref *16* for a general description of the technique). In short, the excitation light was produced by a cavity-dumped dye laser (Coherent 700 with Coherent 7220 Dye Laser Cavity Dumper, dye, Rhodamin 6G), synchronously pumped by a mode-locked frequency doubled Nd:YAG laser (Coherent Antares 76-S). The FWHM of the autocorrelation function of the pulse was about 8 ps. The excitation wavelength was 600 nm. The repetition rate of the dye laser was set to 148 kHz. The excitation light intensity at the sample was kept below 0.5 nJ/(pulse cm^2). Fluorescence of the sample was detected at 90° with respect to the excitation light, using a microchannel plate (MCP) photomultiplier (Hamamatsu R1564U-07) cooled by a thermoelectric cooler (Hamamatsu C2773). The experiment proceeded until at least 10 000 counts at the initial maximum of the decay were collected.

Fluorescence kinetics were deconvoluted using the apparatus response function, obtained by detecting excitation light scattered from a nonfluorescent sample (water solution of milk powder). The FWHM of the apparatus response function of the setup was about 80 ps. The deconvoluted decay curves were fitted by a sum of exponents representing different fluorescence lifetimes.

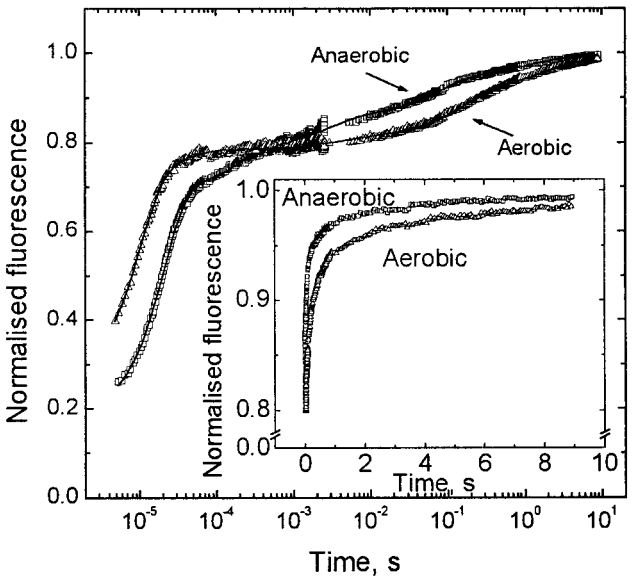

FIGURE 1: Fluorescence quenching in LHCII aggregates after strong 590 nm laser pulse excitation under aerobic (open triangles) and anaerobic (open squares) conditions. Solid lines represent multiexponential fits according to eq 1. Parameters of the fit are presented in Table 1. The fluorescence before $t = 0$ is normalized to 1. Note the logarithmic time scale. Insert, slower part of the kinetics shown on a linear time scale.

RESULTS

ΔF at Room Temperature; Effect of Oxygen. Fluorescence intensity changes were observed after excitation of LHCII aggregates with an intense nanosecond laser pulse (Figure 1). The overall fluorescence quenching starts within less than 4 μs after the laser pulse excitation (response time of the setup) and proceeds over more than 7 orders of magnitude in time, demonstrating different quenching efficiencies at various times. The measurements were carried out under aerobic and anaerobic conditions, since oxygen is known to influence the decay times of Chl and Car triplet states (*17*, *14*) (Figure 1). To reveal the differences in the kinetics measured under aerobic and anaerobic conditions, and to get "orientating values" for the quenching parameters on the different time scales, the fluorescence recovery kinetics normalized to the initial fluorescence yield (without light-induced quencher) were fitted with the time-dependent Stern−Volmer equation (eq 1, see Appendix 1). It was assumed that the lifetime of the excitation in the aggregate is determined mainly by the quenchers, generated by the initial strong laser pulse, and the quenchers are sufficiently separated from each other not to interact, thus, that each of the quenching states decays independently with an exponential decay.

$$\frac{\Phi}{\Phi_0} = \frac{1}{1 + \sum_i A_i \, e^{-t/\tau_i}} \qquad (1)$$

Φ and Φ_0 correspond to the time dependent and the initial fluorescence yield, respectively. $A_i = (k_i/k_{fl} + k_{nr})(q_i(0))$ where k_{fl} is the radiative excitation decay rate, k_{nr} is the intrinsic rate of radiationless decay, k_i is the excitation decay rate due to the trapping by the ith quencher the initial concentration of which is determined by $q_i(0)$, and τ_i is the decay time of the ith light-induced quencher. For a satisfactory fitting of the experimental curves shown in Figure 1, $i = 6$ was needed. One of the lifetimes (τ_6) represents the disappearance of the longest-lived quenchers that last much longer than the time range of our experiments and it is assumed to be infinitely long (see also ref *13*). The parameters revealed by this analysis are shown in Table 1.

A fast decaying strong quenching stage, during which up to about 80% of the fluorescence is quenched is seen at initial times. Its time scale and oxygen dependence are similar to those observed by laser flash-induced triplet minus singlet (T−S) absorption difference measurements and resemble the behavior of Car triplets (*17*, *14*, *5*). As has already been observed before, the decay of Car triplets under aerobic conditions becomes faster (*4*) and non monoexponential (*14*) and at the time when the measurement is started (4 μs after excitation pulse), more triplets have already been lost in the presence of oxygen. This allows to explain the differences in the initial amplitudes A_1 and the lifetimes τ_1 in Table 1.

On a millisecond time scale, the behavior of the fluorescence recovery under aerobic and anaerobic conditions is very different: under anaerobic conditions the recovery is clearly observed, whereas under aerobic conditions no significant change can be distinguished for "a while". This results in more pronounced quenching under aerobic conditions on longer time scales. The final (millisecond to second) stages decay faster under anaerobic conditions (see also insert of Figure 1). The longest time scales, on which the recovery of fluorescence proceeds, are of the order of several seconds and there is some residual quenching left 10 s after the excitation pulse. Although there still remains to determine the correlation between our observations with pulsed excitation light and previous experiments under continuous illumination conditions (*9*, *10*, *13*), slow phases (of the order of seconds) in fluorescence recovery indicate that pulse-induced quenching can be of physiological importance.

ΔF at 77 K. Measurements of the laser pulse induced fluorescence quenching were also carried out at low temperature. The fluorescence recovery kinetics at room temperature and 77 K are compared in Figure 2 and the fitting parameters of the kinetics at 77 K are presented in Table 1. By lowering the temperature from 295 to 77 K, two initial lifetimes increase from 8 to 13 μs and from 90 to 148 μs, respectively. The lifetime of the Car triplet observed by T−S absorption difference spectroscopy at 77 K (*14*) is also 13 μs and does not depend on the concentration of oxygen (results not shown, see also ref *17*). The long-lived quenchers decay very slowly at 77 K (Table 1). It turned out that after a series of laser pulses (20 pulses at 1 Hz), the amount of light-induced long-lived quenching was saturated, remaining approximately unchanged at the level where up to 25% of the initial fluorescence was quenched for more than 45 min (data not shown). The fact that at low temperatures it is possible to keep the light-induced quenching capacity for long times, allowed us to perform experiments that are more time-consuming (e.g., steady-state spectroscopic measurements or time-resolved experiments that require a lot of averaging).

Fluorescence Lifetimes before and after the Generation of Light-Induced Quenchers. For a more detailed study of the origin of the quenchers and for obtaining the values of the trapping rates k_i (eq 1), fluorescence lifetimes of LHCII

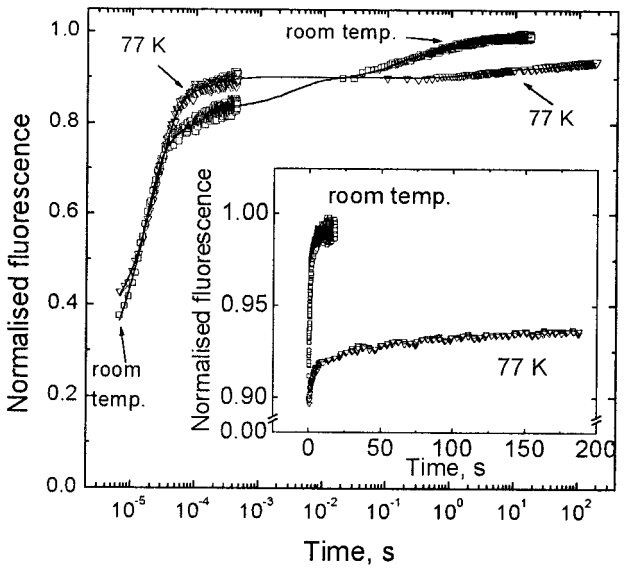

FIGURE 2: Laser flash-induced fluorescence kinetics of LHCII aggregates at room temperature (open squares) and at 77K (open triangles). Solid lines represent multiexponential fit according to eq 1. Parameters of the fit are presented in Table 1. Insert, the slower part of the kinetics shown on the linear time scale.

Table 1: Decay Parameters of Light-Induced Fluorescence Quenching in LHCII Aggregates under Aerobic and Anaerobic Conditions at Room Temperature and 77 K[a]

	aerobic, 295 K		anaerobic, 295 K		aerobic, 77 K	
i	A_i	τ_i	A_i	τ_i	A_i	τ_i
1	2.73	5.4 μs	4.26	9.9 μs	1.96	13.8 μs
2	0.13	32 μs	0.19	163 μs	0.074	148 μs
3	0.04	3.9 ms	0.11	2.5 ms	0.02	2.9 s
4	0.14	149 ms	0.11	72 ms	0.016	38 s
5	0.08	1.70 s	0.05	1.3 s	0.074	1906 s
6	<0.015	∞	<0.005	∞		

[a] The results were obtained by fitting experimental data of Figure 1 and Figure 2 with eq 1. The standard errors of the fit do not exceed 10% of the obtained values.

aggregates were measured using the single-photon-timing technique. The measurements were performed at 77 K, since at this temperature it is possible to "trap" light-induced quenchers for a time period long enough to perform this type of experiment (see Figure 2). Fluorescence kinetics were collected from a dark-adapted sample, then the sample was irradiated by a series of intense ns laser pulses, up to the saturation level where about 25% of the initial fluorescence was quenched and the fluorescence kinetics were recorded again. The results are shown in Figure 3. As is seen from the experimental data and the fitting parameters presented in Table 2, the light-induced drop in fluorescence yield appears due to the reduced lifetime of the excited state and not due to the decreased number of emitting chromophores. Shortening of fluorescence lifetimes due to irreversible and slowly decaying (on the order of minutes) light-induced quenchers was previously observed at room temperature (*9*). The average fluorescence lifetimes in our measurements (Table 2) are longer than the fluorescence lifetimes published elsewhere (*18*, *19*), most likely, becuase LHCII was isolated in the dark from dark-adapted leaves. Exposure of LHCII to the light generates additional quenchers. In addition, high repetition laser pulses lead to accumulation of triplets, as is evident from Figures 1 and 2. In our samples, we were

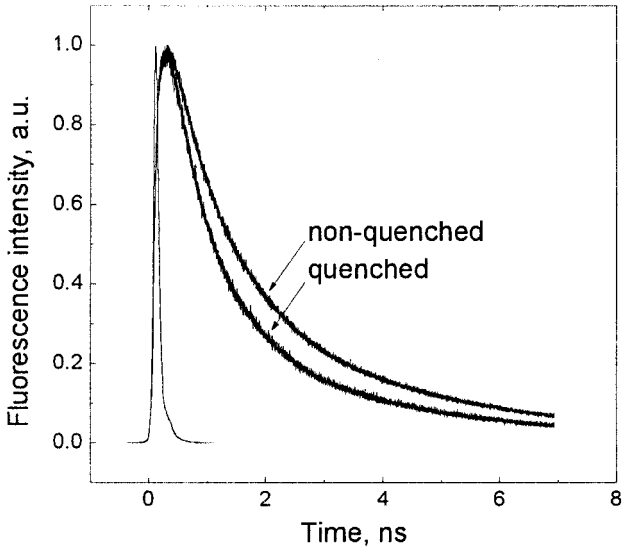

FIGURE 3: Fluorescence decays at 77K before and after generation of long-lived fluorescence quenchers by a series of intense ns laser pulses. The apparatus response function of the setup, measured for a scattering nonfluorescent sample is also shown. The kinetics were normalized in the maximum.

able to reproduce similar lifetimes as published in refs *18* and *19* with a 4 MHz laser pulse repitition rate (data not shown).

The third lifetime T_3 was determined from a free fit with three exponentials for both traces. It turned out to be approximately the same. T_3 represents the intrinsic excited-state lifetime of Chl in the protein, or, in other words, the excited-state lifetime in LHCII aggregates without quenchers. The T_3 was fixed at the determined value of 4.1 ns for further fitting of both data sets. The fluorescence kinetics of the dark-adapted samples is biexponential. The lifetime T_2 should be attributed to domains containing permanent quenchers. The lifetime T_{1q} appears in the fluorescence kinetics when the sample is excited by ns laser pulses and represents light-induced quenchers. The ratio of the fluorescence quantum yields before (Φ_0) and after excitation of the sample (Φ_q) can be estimated according to

$$\frac{\Phi_q}{\Phi_0} = \frac{[A_{1q}T_{1q} + A_{2q}T_{2q} + A_{3q}T_{3q}]}{[A_2T_2 + A_3T_3]} \qquad (2)$$

where A_i and T_i are the values given in Table 2. This gives $\Phi_q/\Phi_0 = 0.76$, i.e., the value calculated from the lifetimes is in good agreement with the experimentally observed amount of fluorescence quenching (25%). The fact that the fluorescence kinetics itself is not monoexponential can be attributed to the heterogeneity of the LHCII macroaggregates.

ΔF at Different States of LHCII Aggregation. The influence of aggregation on ΔF was investigated by recording kinetic traces at different DM concentrations. The time-dependence of the traces in the ms-s time range did not differ very much for various levels of aggregation (data not shown see also ref *13*); however, the overall size of the quenching effect decreased with desaggregation (Figure 4). For estimations, the integrated area between the line, where the normalized fluorescence is equal to one, and the measured curve of normalized fluorescence was taken as a measure of the degree of quenching. The integration range was taken

Table 2: Fluorescence Lifetimes of LHCII Aggregates at 77 K before and after Generation of the Quenchers by Strong Laser Pulses[a]

without light-induced quenchers		with light-induced quenchers	
amplitudes	lifetimes	amplitudes	lifetimes (ps)
		$A_{1q} = 0.6 \pm 0.03$	$T_{1q} = (800 \pm 43)$ ps
$A_2 = 0.7 \pm 0.038$	$T_2 = (1100 \pm 59)$ ps	$A_{2q} = 0.2 \pm 0.011$	$T_{2q} = (1160 \pm 63)$ ps
$A_3 = 0.3 \pm 0.016$	$T_3 = (4100 \pm 220)$ ps	$A_{3q} = 0.2 \pm 0.011$	$T_{3q} = 4100$ ps

[a] The data were fitted with three exponentials, however for the data set measured before generation of the long-lived quencher two of the three lifetimes turned out to be the same. They are represented by A_2 and T_2 in the table. The error bars reflect standard errors of the fit.

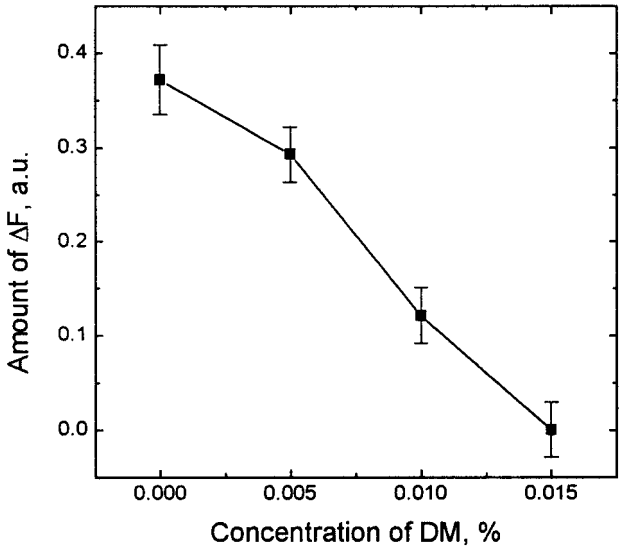

FIGURE 4: The dependence of light-induced fluorescence quenching on the concentration of DM. The amount of quenching at each concentration of DM is calculated from the graph (similar to one in the insert of Figure 1) by integrating the area between the level of initial fluorescence and the measured trace over the time interval from 5 ms to 18 s.

from 5 ms to 18 s (the range is presented in the insert of Figure 1). Above the CMC the ΔF becomes undetectable. This is in agreement with previous results using continuous illumination conditions (*13*).

DISCUSSION

Fluorescence Recovery Kinetics after Laser Pulse Excitation. The approach of eq 1 is evidently applicable to homogeneous systems with independent quenchers generated immediately upon laser excitation. This equation can be generalized for any temporal behavior of quenchers as long as the time scales of quencher evolution are much longer than the excited-state lifetime:

$$\frac{\Phi}{\Phi_0} = \frac{1}{1 + \sum_i \kappa_i q_i(t)} \qquad (3)$$

where $\kappa_i = k_i/(k_{fl} + k_{nr})$ is the relative quenching rate (in comparison with the intrinsic decay rate of excitations see Appendix for exact definitions), while $q_i(t)$ is not necessarily an exponential decay function and its time dependence can vary, depending on the model applied.

The observations in our experiments (see Figure 1 and Table 1) combined with other data (*17*, *20*, *21*, *14*, *5*) clearly confirms the fact that Car triplets act as one type of quencher, having a lifetime of the order of 10 μs and being responsible

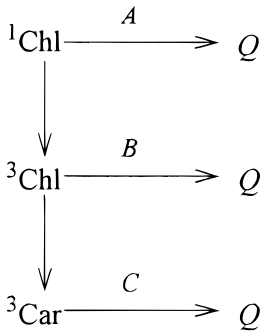

FIGURE 5: Schematic view of possible pathways for quencher formation in LHCII following the excitation of Chl *a*.

for the initial strong quenching stage. The second quencher in LHCII, as judged from a comparison of the measured lifetime of hundreds of microseconds (Table 1) to the lifetimes of Chl triplets (*17*, *14*, *5*), is most likely a Chl triplet. Although most of the Chl triplets are transferred to Cars (*4*), some Chl triplets have been observed in LHCII at 77K (*17*, *14*) and at room temperature (*5*). This implies, that some of the Chls *a* in LHCII are not in contact with Cars as was also suggested by the modeling of spectroscopic experimental data (*22*, *23*). Triplet states of these Chls apparently quench fluorescence showing that they are connected to the main bulk of Chls and do not originate from the contaminated, free or partially decoupled Chls, which are obtained at high detergent concentrations (*24*). We found that the generation of Chl and Car triplets starts to saturate at 10−15% of the maximum intensities used in this work. This is mainly due to singlet−singlet annihilation in LHCII domains. However, the intensity dependence of the amount of Chl and Car triplets is practically the same, excluding the possibility of generating extra Chl triplets due to overexcitation of the system.

The long-lived quenching (longer than a few milliseconds) cannot be explained on the basis of Car triplets since they only live microseconds or Chl triplets since their lifetime under anaerobic conditions ranges from 600 μs to 1.1 ms (*2*, *4*). In general, the formation of light-induced long-lived quenchers *Q* can proceed via the channels depicted in Figure 5. A quencher *Q* might be produced by the direct photoreaction from the singlet excited state of a Chl molecule (from ^{1}Chl via channel A, Figure 5). However, the channel A does not provide an obvious way to explain the oxygen dependence of light-induced quenching, because the oxidation of singlet excited Chls has a low probability due to the short lifetime of the Chl excited state, and due to differences in spin multiplicity of the Chl singlet excited state and the triplet state of ground-state oxygen. There is no experimental evidence that singlet excited Chl can interact with oxygen. For these reasons we assume that the intersystem crossing

pathway leading to a creation of Chl triplets (^{3}Chl, Figure 5) is the major route toward quencher formation.

The transfer efficiency of triplets from Chl to Car has been reported to be 92 ± 7% in LHCII (*5*). So, even though the majority of Chl triplets are transferred to Cars, the remaining Chl triplets should also be considered. There are two possibilities: (i) the quencher is generated from Car triplets (from ^{3}Car via channel C, Figure 5), or (ii) the quencher is generated from Chl triplets (channel B). Previously, the long-lived light-induced fluorescence quenching was attributed to cis-trans isomerization of a violaxanthin/neoxanthin molecule in its triplet state (*11*). We have not been able to observe any ns laser flash induced absorption changes on the microsecond to millisecond time scale around 345 nm (data not shown), which are characteristic for cis isomers of Car. In addition, the putative isomerization pathway does not provide an explanation why on millisecond to second time scales quenching is stronger under aerobic conditions (Car triplets decay faster in the presence of oxygen thus the accumulated amount of trans isomers should be smaller under those conditions). Also, the energy of a Car triplet is relatively low (even insufficient to excite the oxygen molecule) and the range of any other possible products accessible from the Car triplet state is very much limited by this fact. On the basis of the above considerations and experimental facts, we conclude that the long-lived quenchers *Q* (on the millisecond to second time scale) are generated from Chl triplets (channel B). Chl triplets effectively react with ground-state oxygen bringing it to the singlet excited state which turns oxygen into a very reactive oxidizing agent (*2*). In addition, if we assume that the long-lived quenchers result from the oxidation reactions performed by singlet oxygen, we obtain a consistent explanation for the different behavior of the fluorescence recovery kinetics under aerobic and anaerobic conditions. Note, that under anaerobic conditions long-living quenchers are still generated quite efficiently (see Figure 1) which indicates that they can also be generated without the presence of oxygen. Thus, the oxygen must be an additional factor enhancing the conversion of Chl triplets to long-lived quenchers. Appendix 2 illustrates the hypothesis how long-lived quenchers can be produced in LHCII from Chl triplet states. The model describes well the time evolution and oxygen dependence of light-induced fluorescence quenching on early time scales up to several tens of milliseconds. The obtained lifetimes of Car and Chl triplet decay are consistent with those reported in the literature (*4*, *14*). Parameters obtained from the model are defined in Appendix 2 and their values are given in Table 3.

The long-lived quenchers generated from Chl triplets can only be observed at high light intensities, where the accumulation of Chl triplets becomes significant. At low light-intensities, light-induced quenchers have been observed at room temperatures, but not at 77 K (*25*). In our experiments, light-induced quenching is present at 77 K (see Figure 2, Table 1), however, it is weaker than at room temperature. On the time scales of seconds many processes, e.g., light-induced structural changes (*26*, *25*), can take place that can give different contributions to long-lived quenching at room temperature.

Possible Origin of Oxygen-Dependent Light-Induced Quenching. Pigment radicals are the most probable candidates for the oxygen-dependent light-induced quenchers in LHCII. According to our hypothesis (see Appendix 2), they are generated from Chl triplets and their generation partly proceeds via the sensitization of oxygen. Chl radicals are known to be efficient fluorescence quenchers in photosynthetic systems [for example the radical of special pair in the reaction center of photosystem II (*27*, *28*)]. Part of the oxidation reactions may be irreversible (*15*) which is reflected by the larger amplitude of the longest quenching component (τ_6) in the presence of oxygen. Excitation of Chl in organic solvents under anaerobic conditions was shown to produce Chl cations directly from the triplet states of Chl (*29*). The amount of Chl triplet states and Chl cations was diminished in the presence of oxygen (*29*). A similar behavior is observed in this study. The presence of Chl radicals in LHCII was proposed in the study of the Z-band of thermoluminescence (*30*, *31*). Formation of small amounts of radicals upon photoinhibitory illumination was observed in LHCII (*32*). Note, that the evolution (recombination) of radicals can proceed via many stages, sometimes following nonlinear rate laws. All these processes may add up to yield complex recombination kinetics similar to the one observed on millisecond to second time scales (Figure 1).

An interesting (although speculative) analogy with the results of single-molecule spectroscopy and other experiments can be drawn at this point. The observed "blinking" of bacterial light-harvesting complexes as seen by confocal microscopy (*33*) was interpreted in terms of the creation of BChl cation radicals, similar to the ones that we propose for LHCII. Recently, it was shown that carotenoidless LH2 and LH1 complexes from purple bacteria form BChl a cation radicals via BChl triplet states, fully in line with the model proposed above (*34*).

It still remains to be investigated how much quenchers generated by Chl triplet take part in the protection of photosynthetic apparatus against overexcitation at high light intensities. Recently, Chl triplets have been observed in chloroplasts under aerobic but not under anaerobic conditions (*35*).

The above-mentioned observations and those of our study indicate that the possibility should seriously be considered that various radicals are involved in the processes of nonphotochemical quenching at high light intensities when the accumulation of Chl triplets becomes significant. It is interesting to note that the creation of radicals provides the photosynthetic system with a negative feedback protection

Table 3: Estimated Model Parameters of Fluorescence Recovery Kinetics[a]

	room temperature		77 K
parameter	anaerobic	aerobic	
$q_{Chl}(0)$	0.91 ± 0.02		0.92 ± 0.01
$q^x_{Chl}(0)$	0.09 ± 0.02		0.08 ± 0.01
$1/r_{Car}$	(9.7 ± 0.8) μs		(14 ± 0.9) μs
$1/r_{Chl}$	(714 ± 48) μs		(706 ± 41) μs
$1/r_{+Q}$	(681 ± 42) μs		(556 ± 37) μs
$1/r_{-Q}$	30 ms		1 s
ξ_{Car}	1	2.2 ± 0.2	1
ξ_{Chl}	1	7.2 ± 0.6	1
ξ_{+Q}	1	11.7 ± 0.9	1
ξ_{-Q}	1	0.275 ± 0.05	1
$\kappa_{Car} = \kappa_{Chl} = \kappa_Q = \kappa$	4.7 ± 0.3		2.1 ± 0.2

[a] The parameters revealed by the fit shown in Figures 7 and 8. The error bars reflect standard errors of the fit.

mechanism. The production of one radical leads to the quenching of singlet excitations, thus decreasing the possibility of production of additional harmful products.

Aggregation Dependence. The effect of long-lived fluorescence quenching becomes undetectable when LHCII aggregates are disassembled into trimers. Previous studies showed that fluorescence and triplet yields increase upon desaggregation (*36*, *5*), but Chl triplet transfer to Car is not affected (*5*). According to our model, this suggests that more long-lived fluorescence quenchers should be produced in desaggregated LHCII. The opposite effect of the long-lived fluorescence quenching can be explained in terms of a reduced size of the quenching domain. When a quencher is generated in a large aggregate, the fluorescence of the whole quenching domain is "switched off", whereas in a trimer it quenches the fluorescence of just one trimer. Let us consider the situation when LHCII is in its trimeric form (DM concentrations above CMC). Then, since the different fluorescence intensities of separate trimers must be summed up to obtain the total fluorescence intensity, the formalism of a homogeneous model can no longer be applied. One triplet generated in a trimer, quenches all singlet excitations thus excluding the possibility to generate another one. As a consequence, the LHCII trimer with a triplet will have a fluorescence yield close to zero. Only the trimers without triplets will fluoresce. Normalizing the fluorescence yield of a sample with triplets present to the fluorescence yield of the same sample without triplets, one finds instead of eq 3:

$$\Phi/\Phi_0 = 1 - \sum_i q_i(t) \tag{4}$$

On a microsecond time scale, when Car triplets are present in LHCII trimers, around 50% of the fluorescence is quenched (data not shown), i.e., approximately half of all trimers have triplets. As can be seen from Table 3, the Chl triplets that are not transferred to Cars make up about 10% of this amount, i.e at approximately 20 μs, only 5% of all fluorescence will be quenched by Chl triplets. Further, we see that about a half of Chl triplets decay via intrinsic decay and the rest participate in the generation of a light-induced quencher (rates r_{Chl} and r_{+Q} in Table 3 are similar). Since only one of the channels leads to further quenching, only ca. 2.5% contributes to the long-lived quenching. This value does not exceed the error bars of Figure 2. Here we considered the parameters obtained under anaerobic conditions. The ones obtained for aerobic conditions give similar results. Upon aggregation of LHCII the triplet yield is lowered several times (*36*, *5*). Despite this effect, the observed amplitude of the long-lived fluorescence quenching indicates that aggregation-induced amplification of the quenching, via an increase of the quenching domain is a significant effect.

CONCLUSIONS

Correlation of the fluorescence recovery kinetics in LHCII measured after excitation by a strong ns laser pulse with similar transient absorption kinetics (*17*, *14*, *5*) show that a small amount of Chl a triplets which is not transferred to Car can quench fluorescence, i.e., they are connected to the main bulk of Chl molecules. Modeling of the fluorescence recovery kinetics illustrates how long-lived fluorescence quenchers can be generated from these Chl triplets. The generation of quenchers is sensitive to the presence of oxygen. It is proposed that long-lived fluorescence quenchers can originate from Chl cations or other radicals which are produced directly from Chl triplets or via Chl triplet sensitized singlet oxygen. The total recovery of the fluorescence is achieved after recombination of the radicals. Aggregation strongly enhances the efficiency of the light-induced fluorescence quenching via an increase of the quenching domain size.

ACKNOWLEDGMENT

We are grateful to Florentine Calkoen for biochemical assistance with the preparation of LHCII.

APPENDIX 1

Fluorescence Yield in Photosynthetic Antennae with Quenchers. The temporal evolution of excitations in a large homogeneous system with quenchers can be described by the following kinetic equation:

$$\frac{dn}{dt} = J - n\sum_i k_i q_i(t) - k_{fl}n - k_{nr}n \tag{5}$$

where J is the generation function of excitations by the measuring light, which creates the excitation population n in the aggregate, k_{fl} is the radiative excitation decay rate, k_{nr} is the intrinsic rate of radiationless decay, k_i is the excitation decay rate due to the trapping by the ith quencher, $q_i(t)$ is the relative concentration of the ith quencher. So far, we do not make any specific assumptions about time dependence of concentrations $q_i(t)$.

Due to the large differences between the time scales of the excitation decay ($1/k_{fl}$, $1/k_{nr}$, and $1/k_i$ are of the order of picoseconds to nanoseconds) and characteristic times of quencher evolution (which in the case under consideration are of the order of microseconds to seconds, see Figure 1), the excitation decay kinetics on the long time scale is determined by the time-evolution of the quenchers and allows to apply quasi-stationary conditions in eq 5. In this case, the fluorescence yield Φ, according to the definitions used in eq 5, is given by

$$\Phi = k_{fl}\frac{n}{J} \tag{6}$$

which in analogy to the Stern−Volmer equation with time-dependent coefficients reflects the slow scale changes in the quencher concentrations. Normalized to the quantum yield of fluorescence when quenchers are absent ($q_i(t) = 0$ for all i), the fluorescence yield in the system with quenchers present is the same as eq 3, where $\kappa_i = \dfrac{k_i}{k_{fl} + k_{nr}}$ is the relative "quenching capacity" of ith quenching channel. Equation 3 is true for homogeneous infinitely large aggregates with time scales of quencher evolution being much longer than the time scales of excitation dynamics.

If the time evolution of a quencher is independent from that of other quenchers and can be represented by the decay time τ_i, i.e.,

$$\frac{dq_i(t)}{dt} = \frac{q_i(t)}{\tau_i} \tag{7}$$

we immediately get eq 1, which is a special case of eq 3. A_i in eq 1 roughly represent the amount of quenching at $t = 0$: $A_i = \kappa_i q_i(0)$.

APPENDIX 2

Hypothetical Model of Light-Induced Quencher Generation from Chl Triplets. On the basis of the fact that not all Chl triplet states are transferred to Cars in our preparations (*17*, *14*, *5*), a general model of quencher generation following pathway B in Figure 5 will be introduced, that allows to interpret qualitatively time and oxygen dependencies of light-induced quenching shown in Figure 1. (The hypothesis underlying this model has been presented in the Discussion section.) The assumptions and definitions of the model are shown in Figure 6 and they are described as follows.

(1) All Chl *a* triplets are divided into two "pools"—the ones which are in close vicinity to Cars and, therefore, lead to triplet transfer to Car molecules (concentration q_{Chl}) and those being further apart from the Car molecules and remain in the triplet state after being created (q^x_{Chl}). The triplet transfer rate $r_{Chl\rightarrow Car}$ from Chl *a* to Car is fast (takes place on a subnanoseconds time scale) (*3*), therefore, in this pool we neglect the lifetime-limited relaxation of these Chl triplets; on the other hand, the triplet transfer rate to Cars is zero for the other pool, where Chl is disconnected from Car.

(2) In the pool where Chl triplets are transferred to Car, the Car triplets (q_{Car}) decay with rate r_{Car}. This process is influenced by the presence of oxygen (*4*, *14*, *15*) and r_{Car} is different under anaerobic and aerobic conditions. This difference is accounted for by multiplying Car triplet decay rate by a phenomenological renormalization coefficient ξ_{Car}. We set it equal to 1 under anaerobic conditions.

(3) In the pool where Chl triplets are not transferred to Car, two pathways are assumed: (a) generation of the long-lived quencher Q with the rate constant r_{+Q}, (b) intrinsic lifetime limited decay with rate constant r_{Chl}.

The generation of the quencher (concentration q_Q) is influenced by oxygen, indicating that at least part of the long-lived quenchers is generated by singlet oxygen, created via Chl triplets. The quenchers Q generated directly from Chl triplets and via oxygen may have a different origin and decay with different lifetimes; however, for simplicity we will consider all quenchers Q to be the same and we account for the oxygen dependence of the fluorescence kinetics by introducing the phenomenological coefficient ξ_{+Q} (also equal to 1 under anaerobic conditions).

Singlet oxygen formation cannot be directly observed under our experimental conditions. The Chl *a* triplet decay via singlet oxygen can be treated as an increased rate of direct relaxation of the triplets to the ground state. Taking this into account, we change the reaction $^3Chl \rightarrow {}^1O_2 \rightarrow$ *Ground* to the reaction $^3Chl \rightarrow$ *Ground* and renormalize the rate r_{Chl} of the latter reaction using another phenomenological coefficient ξ_{Chl} (also equal to one under anaerobic conditions).

(4) The long-lived light-induced quenchers (q_Q) decay with rate constant r_{-Q}. It is evident from earlier experiments (*13*) and Figure 1 that the long-lived (in the range of tens of milliseconds to seconds) quenchers decay with complex, nonexponential kinetics, however, we simplify the model due to the lack of information on the slow (subsecond to second time scale) processes and approximate the long-lived quencher's decay by a single exponent. The quencher decay apparently is also influenced by oxygen which will be accounted for by using the phenomenological coefficient ξ_{-Q} (also equal to 1 under anaerobic conditions).

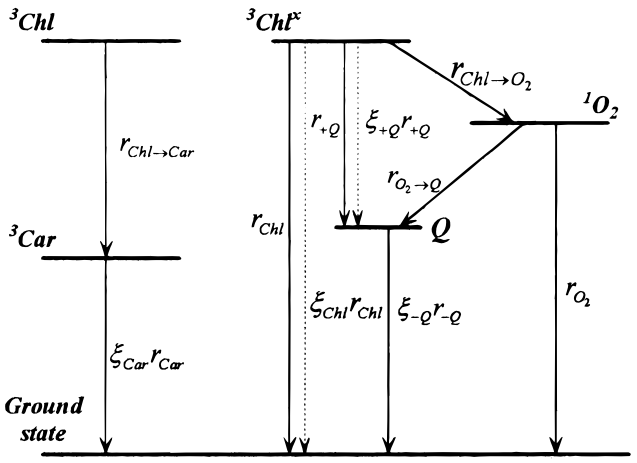

FIGURE 6: Working scheme of Chl triplet decay and generation of long-lived quencher Q in LHCII. ^3Chl and $^3Chl^x$ represent triplets located on Chls with and without neighboring Car, respectively. ^3Car and $^1O_2$ symbolize triplet states of Car and singlet oxygen, respectively. Solid arrows and corresponding rates show the relaxation pathways of the Chl triplets. Dashed lines depict the "effective" reactions to which we change the $^3Chl^x$ reaction with oxygen by renormalizing with the phenomenological coefficients ξ_{Chl} and ξ_{+Q}.

According to the above model, the corresponding kinetic equations are as follows:

$$\frac{dq^x_{Chl}}{dt} = -r_{+Q}\xi_{+Q}q^x_{Chl} - r_{Chl}\xi_{Chl}q^x_{Chl}$$

$$\frac{dq_{Chl}}{dt} = -r_{Chl\rightarrow Car}q_{Chl}$$

$$\frac{dq_{Car}}{dt} = r_{Chl\rightarrow Car}q_{Chl} - r_{Car}\xi_{Car}q_{Chl}$$

$$\frac{dq_Q}{dt} = r_{+Q}\xi_{+Q}q^x_{Chl} - r_{-Q}\xi_{-Q}q_Q \tag{8}$$

The solution of eq 8 yields

$$q^x_{Chl}(t) = q^x_{Chl}(0)e^{-r_x t}$$

$$q_Q(t) = \frac{r_{+Q}\xi_{+Q}q^x_{Chl}(0)}{r_{-Q}\xi_{-Q} - r_x}(e^{-r_x t} - e^{-r_{-Q}\xi_{-Q}t})$$

$$q_{Car}(t) = q_{Chl}(0)\, e^{-r_{Car}\xi_{Car}t} \tag{9}$$

where $r_x = r_{+Q}\xi_{+Q} + r_{Chl}\xi_{Chl}$

Thus, the main quenchers in the system are the Chl and Car triplet states as well as the long-lived quenchers Q. The time evolution of these quenchers is given by eq 9 and by substituting these into eq 3 the simulation of the experimental curves shown in Figure 1 can be undertaken.

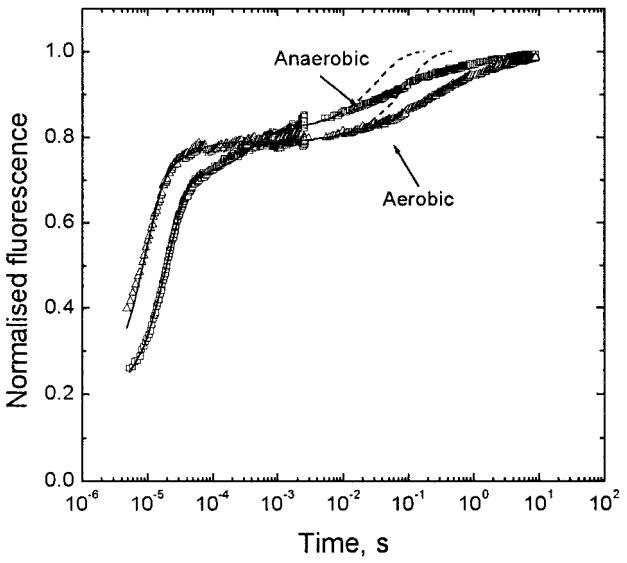

FIGURE 7: Comparison of simulation (solid lines) and experimental results (open symbols) of the fluorescence recovery kinetics in LHCII aggregates after laser pulse excitation under aerobic (triangles) and anaerobic (squares) conditions. The slow part of the simulated kinetics which could not be modeled are shown with dashed lines. Room-temperature measurements.

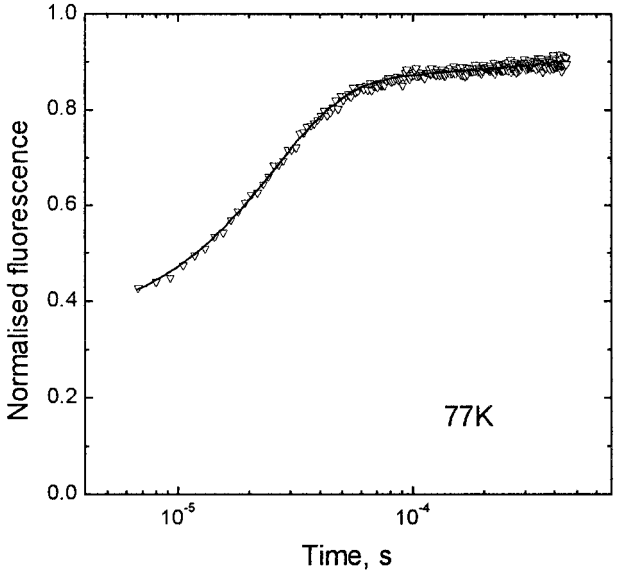

FIGURE 8: Comparison of simulation (solid line) and experimental results (open symbols) of the initial part of fluorescence recovery kinetics after laser pulse excitation in LHCII aggregates at 77 K.

Let us now discuss the possible values of the previously defined relative quenching rates κ_i governing the "quenching capacity" of the *i*th quenching channel (see eq 3). The parameters that follow from the fit are not κ_i themselves, but the products of κ_i and $q_i(0)$ (here different *i* stand for Car and Chl triplets and long-lived quenchers). To interpret those parameters in terms of initial concentrations, we need an assumption about the quenching efficiencies of the various quenchers. The amount of Chl triplets from which the evolution of the quenchers starts is low compared to the total number of pigments. Assuming that the corresponding quenching processes are migration limited (*37*, *38*), κ_{Chl}, κ_{Car}, and κ_Q must be approximately equal, i.e., $\kappa_{Chl} = \kappa_{Car} = \kappa_Q = \kappa$. In case the model works well, this assumption allows us to estimate approximately the fraction of the Chls which are not in the contact with Cars in LHCII. To ensure this, we use the fitting constraint that $q^x_{Chl}(0) + q_{Chl}(0) = 1$, which means that fractions of Chl triplets in contact with Cars and those disconnected from Cars are directly obtained from the fit.

Relatively good correspondence between the simulated and measured curves is achieved for the early kinetics up to 30 ms time range (Figure 7); the main features of the two kinetic traces—initial course during Car/Chl triplet quenching stage and the crossing point due to different behavior under aerobic and anaerobic conditions—have been reproduced by the model. The later stages could not be modeled satisfactory due to the simplifying assumption of monoexponential decay of long-lived quenchers.

The parameters of the simulation are given in Table 3. The estimated fraction of Chls that is not in contact with Cars is $q^x_{Chl} = 0.09$. This would mean that one Chl *a* out of 11 does not transfer its triplet to carotenoid, which is in agreement with the results of T−S measurements on similar preparations (*5*). Knowing that there are 7 or 8 Chls *a* per LHCII monomer (*39*, *40*), the rough estimation would be that on average two Chls *a* per LHCII trimer are not in contact with a carotenoid. This result is at variance with the Kühlbrandt's original assignment of Chls in LHCII monomer (*39*) and is in line with the assignment based on the modeling of spectroscopic experimental data (*22*, *23*).

The Car triplet lifetimes (9.7 μs under anaerobic conditions, 4.4 μs under aerobic conditions) are in good agreement with other experimental data (*4*, *14*, *15*). The small discrepancy between the simulation and the experimental data on the Car triplet time scale arises because we did not account for the previously observed fact, that under aerobic conditions at least two different spectral forms of Car triplets occur, each of which decays with its own kinetics (*14*).

The decay of the Chl triplets, that are not quenched by Car, is influenced by oxygen. Direct decay to the ground state is enhanced $\xi_{Chl} = 7.2$ times and the quencher generation rate r_{+Q} is increased by the factor of $\xi_{+Q} = 11.7$. Thus the overall decay of Chl triplets is around 10 times faster under aerobic conditions, however the amount of quenchers generated from Chl triplets increases only slightly due to acceleration of both decay channels. This allows to explain why in the initial study by Jennings et al. (*9*) a very small effect of oxygen on the continuous-light-induced decline in fluorescence was observed.

Fluorescence quenching taking place on a slower time scale could not be simulated with a monoexponential decay (Figure 7, dashed lines). Partly, this may be due to the presence of several forms of long-lived quenchers, disappearance of which could be influenced by the structural changes (*26*, *41*, *25*) of the pigment−protein complex and/or determined by diffusion-limited processes which inherently give nonexponential kinetics. This is in line with the low-temperature experiments (see Figure 3) where structural changes and diffusion are largely restricted in the frozen glycerol-buffer mixtures. Structural changes could also lead to minor alterations in Chl:Car interactions which may result in changes of the fluorescence yield (*24*).

The fast fluorescence quenching kinetics at 77 K could be modeled by considering only one type of light-induced quencher being generated from Chl triplets. The fit of the

decay at 77 K with eq 9 and 3 is presented in Figure 8. The parameters of the fit are shown in Table 3. The ratio of Chls which have contacts with Car and those which do not, is practically the same at 77 K and at room temperature and is consistent with previous observations (*5*) that the efficiency of triplet energy transfer from Chl to Car does not change more than 4% by varying the temperature. At 77 K, the Car and Chl triplet decays become a little bit slower and generation of the quencher slows down a few percent. In contrast, the decay of the quencher slows down by a few orders of magnitude. This clearly indicates that thermal/diffusion reactions are involved in the decay of the quencher.

REFERENCES

1. Horton, P., Ruban, A. V., and Walters, R. G. (1996) *Annu. Rev. Plant. Physiol. Plant. Mol. Biol. 47*, 655−684.
2. Fujimori, E., and Livingston, R. (1957) *Nature 180*, 1036−1038.
3. Schödel, R., Irrgang, K.-D., Voigt, J., and Renger, G. (1998) *Biophys. J. 75*, 3143−3153.
4. Siefermann-Harms, D. (1987) *Physiol. Plantarum 69*, 561−568.
5. Barzda, V., Peterman, E. J. G., Van Grondelle, R., and Van Amerongen, H., (1998) *Biochemistry 37*, 546−551.
6. Simidjiev, I., Barzda, V., Mustardy, L., and Garab, G. (1997) *Anal. Biochem. 250*, 169−175.
7. Briantais, J.-M. (1996) in *Light as Energy Source and Information Carrier in Plant Physiology* (Jennings, R. C., Zucchelli, G., Ghetti, F., and Colombetti, G. Eds.) pp 113−124, Plenum Press, New York.
8. Demmig-Adams, B., and Adams, W. W. 1992 *Annu. Rev. Plant Physiol. Plant Mol. Biol. 43*, 599−626.
9. Jennings, R. C., Garlaschi, F. M., and Zucchelli, G., 1991 *Photosynth. Res. 27*, 57−64.
10. Gruszecki, W. I., Kernen, P., Krupa, Z., and Strasser, R. J. (1994) *Biochim. Biophys. Acta 1188*, 235−242.
11. Gruszecki, W. I., Matula, M., Ko-chi, N., Koyama, Y., and Krupa, Z. (1997) *Biochim. Biophys. Acta 1319*, 267−274.
12. Barzda, V., Vengris, M., Calkoen, F., Van Grondelle, R., and Van Amerongen, H. (1998) in *Photosynthesis: Mechanisms and Effects* (Garab, G., Ed.) Vol. 1, pp 337−340, Kluwer Academic Publishers, The Netherlands.
13. Barzda, V., Jennings, R. C., Zucchelli, G., and Garab. G. (1999) *Photochem. Photobiol. 70*, 751−759.
14. Peterman, E. J. G., Dukker, F. M., Van Grondelle, R., and Van Amerongen, H. (1995) *Biophys. J. 69*, 2670−2678.
15. Siefermann-Harms, D., and Angerhofer, A. (1998) *Photosynth. Res 55*, 83−94.
16. Holzwarth, A. R. (1995) *Methods Enzymol. 246*, 334−362.
17. Mathis, P., Butler, W. L., and Satoh, K. (1979) *Photochem. Photobiol. 30*, 603−614.
18. Mullineaux, C. W., Pascal, A. A., Horton, P., and Holzwarth, A. R. (1993) *Biochim. Biophys. Acta 1141*, 23−28.
19. Vasil′ev, S., Irrgang, K.-D., Schrotter, T., Bergmann, A., Eichler, H.-J., and Renger, G. (1997) *Biochemistry 36*, 7503−7512.
20. Den Haan, G. A., Warden, J. T., and Duysens, L. N. M. (1973) *Biochim. Biophys. Acta 325*, 120−125.
21. Sonneveld, A., Rademaker, H., and Duysens, L. N. M. (1980) *Biochim. Biophys. Acta 593*, 272−289.
22. Trinkunas, G., Connelly, J. P., Müller, M. G., Valkunas, L., and Holzwarth, A. R. (1997) *J. Phys. Chem. B 101*, 7313−7320.
23. Gradinaru, C. C., Özdemir, S., Gülen, D., Van Stokkum, I. H. M., Van Grondelle, R., and Van Amerongen, H. (1998) *Biophys. J. 75*, 3064−3077.
24. Naqvi, R. K., Javorfi, T., Melo, T. B., and Garab, G. (1999) *Spectrochim. Acta, Part A 55*, 193−204.
25. Gruszecki, W. I., Grudzinski, W., Matula, M., Kernen, P., and Krupa, Z. (1999) *Photosynth. Res. 59*, 175−185.
26. Barzda, V., Istokovics, A., Simidjiev, I., and Garab, G. (1996) *Biochemistry 35*, 8981−8985.
27. Den Haan, G. A., Duysens, L. N. M., and Egberts, D. J. N. (1974) *Biochim. Biophys. Acta 368*, 409−421.
28. Sonneveld, A., Rademaker, H., and Duysens, L. N. M. (1979) *Biochim. Biophys. Acta 548*, 536−551.
29. Imura, T., Furutsuka, T., and Kawabe, K. (1975) *Photochem. Photobiol. 22*, 129−134.
30. Noguchi, T., Inoue Y., and Sonoike, K. (1993) *Biochim. Biophys. Acta 1141*, 18−22.
31. Hagen, C., Paskal, A. A., Horton, P., and Inoue, Y. (1995) *Photochem. Photobiol. 62*, 514−521.
32. Hideg, E., and Vass, I. (1995) *Photochem. Photobiol. 62*, 949−952.
33. Bopp, M.A., Jia, Y., Li, L., Cogdell, R. J., and Hochstrasser, R. M. (1997) *Proc. Natl. Acad. Sci. U.S.A. 94*, 10630−10635.
34. Limantara, L. Fujii, R., Zhang, J.-P., Kakuno, T., Hara, H., Kawamori, A., Yagura, T., Cogdell, R. J., and Koyama, Y. (1998) *Biochemistry 37*, 17469−17486.
35. Javorfi, T., Garab, G., and Naqvi, R. (1999) *Spectrochim. Acta, Part A 56*, 211−214.
36. Naqvi, R. K., Melo, T. B., Raju, B. B., Javorfi, T., Simidjiev, I., and Garab, G. (1997) *Spectrochim. Acta, Part A 53*, 2659−2667.
37. Gillbro, T., Sandström, A., Spangfort, M., Sundström, V., and van Grondelle, R. (1988) *Biochim. Biophys. Acta 934*, 369−374.
38. Barzda, V., Garab, G., Gulbinas, V., and Valkunas, L. (1996) *Biochim. Biophys. Acta 1273*, 231−236.
39. Kühlbrandt, W., Wang, D., and Fujiyoshi, Y. (1994) *Nature 367*, 614−621.
40. Jansson, S. (1994) *Biochim. Biophys. Acta 1184*, 1−19.
41. Simidjiev, I., Barzda, V., Mustardy, L., and Garab, G. (1998) *Biochemistry 37*, 4169−4173.

BI992826N